

## Comprehensive Invasive and Noninvasive Approach to the Right Ventricle–Pulmonary Circulation Unit State of the Art and Clinical and Research Implications

Hunter C. Champion, MD, PhD; Evangelos D. Michelakis, MD; Paul M. Hassoun, MD

*... And I ask, as the lungs are so close at hand, and in continual motion, and the vessel that supplies them is of such dimensions, what is the use or meaning of this pulse of the right ventricle? And why was nature reduced to the necessity of adding another ventricle for the sole purpose of nourishing the lungs?*

—William Harvey, *Exercitatio Anatomica de Motu Cordis et Sanguinis in Animalibus*, 1628

There is still no answer to William Harvey's rhetorical question. He included the right ventricle (RV), its "pulse," the large pulmonary arteries (PAs), and the lungs in the same sentence, emphasizing the concept of a "unit." Although Harvey realized the importance of the RV and its interactions with the pulmonary circulation, 4 centuries later, the RV is largely understudied. At the same time, there has been significant progress in our understanding of the pathology of pulmonary vascular disease and, over the past few years, an explosion of clinical therapeutic trials for PA hypertension (PAH).<sup>1</sup> This unbalanced approach has generated a number of problems and controversies. For example, it is now becoming apparent that even if experimental therapies improve or reverse PAH pathology, this does not necessarily lead to clinical improvement and prolonged survival unless accompanied by a parallel improvement in RV function. The degree of pulmonary hypertension (ie, PA pressure [PAP]) does not strongly correlate with symptoms or survival, whereas RV mass and size and right atrial pressure reflect functional status and are strong predictors of survival.<sup>2</sup> The 6-minute walk test, used as the primary end point in most PAH clinical trials, correlates better with RV function (ie, cardiac output) than with the degree of pulmonary pressure elevation. However, this test is being heavily criticized because of multiple inherent problems and the fact that it does not provide information on specific components of RV–pulmonary vascular function.<sup>3</sup> Although therapies aiming at reversing pulmonary vascular remodeling might also have a positive effect on the RV (eg, sildenafil, which has been

shown to increase RV inotropy<sup>4</sup> and decrease RV hypertrophy,<sup>5</sup> in addition to its effects on the pulmonary circulation), others might have untoward effects on the RV. For example, imatinib, an antiproliferative/proapoptotic agent that shows preliminary promise in reversing pulmonary vascular remodeling,<sup>6</sup> is potentially associated with primary negative (ie, proapoptotic) effects on the myocardium.<sup>7</sup>

As our knowledge of RV physiology and biology increases, it is becoming apparent that a comprehensive approach to the RV, the pulmonary circulation, and their interactions will be beneficial in both clinical management of PAH patients and clinical research. The evolution of RV pathology from the normal to a compensated (hypertrophied) and then decompensated state parallels the evolution of pulmonary vascular pathology from a vasodilated high-capacitance state to vasoconstricted arteries and early loss of endothelial cells/capillaries to an end-stage proliferative and obliterative vascular remodeling (Figure 1). Therefore, it is important to study the RV and the PAs comprehensively and simultaneously as a unit. Here, we discuss standard clinical tests (eg, right heart catheterization and echocardiography) and evolving technologies (eg, magnetic resonance [MR] imaging [MRI] and positron emission tomography [PET]) that have the ability to study the RV–proximal PAs–PA microcirculation unit comprehensively and provide quantitative data. Such data promise to be very relevant to the clinical management of PAH patients and might prove to be ideal end points for future clinical research.

### Hemodynamic Assessment of RV Function and Ventricular-Vascular Interactions

#### Standard Hemodynamic Approaches

Cardiac catheterization remains the gold standard for diagnosing pulmonary hypertension, assessing disease severity, and determining prognosis and response to therapy. By directly measuring pressures and indirectly measuring flow, right heart catheterization allows determination of prognostic

From the Pulmonary Vascular Disease Center, Department of Medicine, University of Pittsburgh Medical Center, Pa (H.C.C.); Pulmonary Hypertension Program and Division of Pulmonary and Critical Care Medicine (P.M.H.), Johns Hopkins Medical Institutions, Baltimore, Md; Pulmonary Hypertension Program, Department of Medicine (Cardiology), University of Alberta, Alberta, Edmonton, Canada (E.D.M.); and Pulmonary Vascular Research Institute, Chicago, Ill (H.C.C., E.D.M., P.M.H.).

Guest Editor for this article was John H. Newman, MD.

Correspondence to Hunter C. Champion, MD, PhD, FAHA, FFPVRI, Visiting Assistant Professor of Medicine, Division of Pulmonary, Allergy, and Critical Care Medicine, Department of Medicine, University of Pittsburgh Medical Center, NW628 Montefiore Hospital, 3459 Fifth Avenue, Pittsburgh, PA 15260. E-mail: championhc@upmc.edu

(*Circulation*. 2009;120:992-1007.)

© 2009 American Heart Association, Inc.

*Circulation* is available at <http://circ.ahajournals.org>

DOI: 10.1161/CIRCULATIONAHA.106.674028

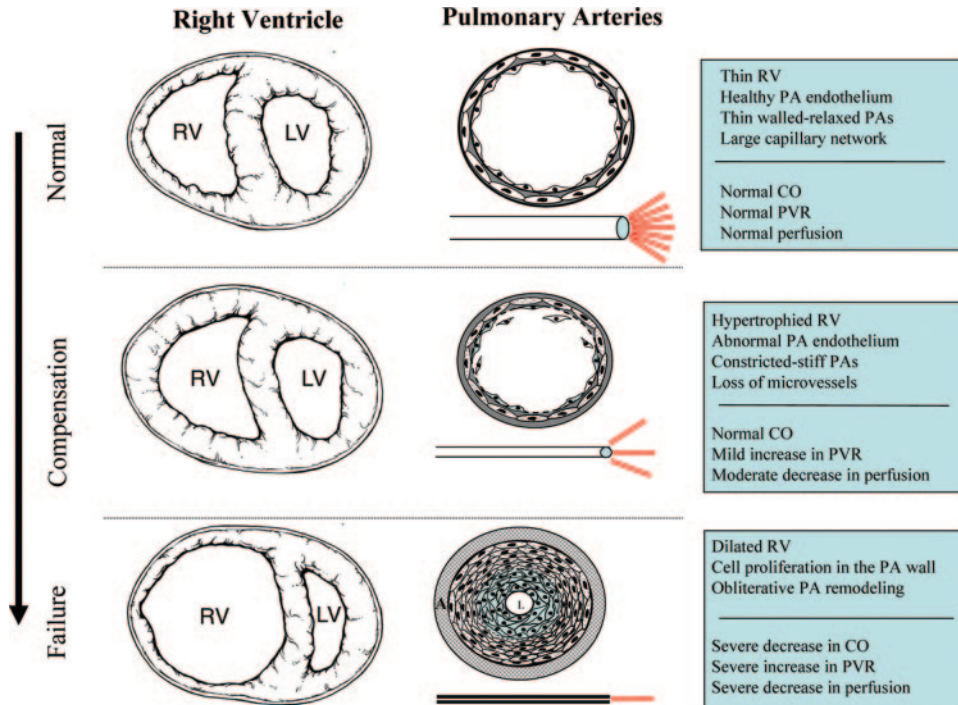


**Figure 1.** Schematic showing the theoretical progression of pulmonary vascular disease and the subsequent effect on RV function from normal physiological conditions (top) to severe pulmonary vascular remodeling and subsequent RV failure (bottom). Note that in the compensated state clinical studies as currently used might miss the disease because in that stage cardiac output (CO) is preserved (ie, no symptoms) and the hemodynamics are minimally if at all affected. In contrast, accurate measurements of the RV mass, PA stiffness, or lung perfusion, as discussed in this review, might clearly identify this stage of disease.

markers such as right atrial pressure, cardiac output, and mean PAP.<sup>8</sup> Importantly, this procedure has been shown to be safe, with no deaths reported in the National Institutes of Health registry study<sup>8</sup> and a recent study showing a procedure-related mortality of 0.055%.<sup>9</sup> Right heart catheterization determines the presence or absence of pulmonary hypertension, may allow definition of the underlying cause, and allows prognostication. The most critical aspect to right heart catheterization is that it should be performed appropriately and the data interpreted with accuracy and precision. Because the end-expiratory intrathoracic pressure most closely correlates with atmospheric pressure, it is important that all RV, PA, pulmonary wedge, and left ventricular (LV) pressures be measured at end expiration.<sup>10–12</sup> This is especially true in patients in whom there can be significant variation between inspiratory and end-expiratory vascular pressures (obese patients and patients with intrinsic lung disease). After determination of the presence of pulmonary hypertension, pulmonary venous pressures should be evaluated by the pulmonary capillary wedge pressure (PCWP). PAH is defined by a PCWP of  $\leq 15$  mm Hg at rest or with exertion to exclude LV dysfunction, mitral valve disease, or other conditions of pulmonary venous hypertension.<sup>12,13</sup> This value was based on the normal PCWP or LV end-diastolic pressure of  $< 8$  mm Hg and the observation that 2 SDs above a normal PCWP is  $\approx 14$  mm Hg.<sup>14</sup> It is important to note, however, that a PCWP of 14 or 15 mm Hg is still not normal.

For the measurement of cardiac output, both thermodilution and Fick methods are reliable in PAH patients, except those with severe tricuspid regurgitation or cardiogenic

shock.<sup>15</sup> Vasodilator challenges with inhaled nitric oxide or intravenous epoprostenol or adenosine are encouraged in all patients at the time of diagnosis and in follow-up studies.<sup>3</sup> A favorable vasodilator response is defined by consensus as a drop in mean PAP of at least 10 mm Hg to a value  $\leq 40$  mm Hg with an unchanged or increased cardiac output.<sup>16</sup> Below, we discuss a number of tests that can complement the standard procedure and provide critical data on the condition of the RV-PA unit.

### Confrontational Testing to Assess Pulmonary Circulation-RV Interactions

Some patients with pulmonary vascular disease are not symptomatic at rest but have symptoms with exertion. This observation provides a potential for exercise or volume challenge during right heart catheterization to better diagnose early pulmonary vascular disease. In patients with risk factors for nonsystolic LV dysfunction (sleep-disordered breathing, systemic hypertension, obesity, diabetes/glucose intolerance), one should consider confrontational testing (to uncover potential increases in PCWP) by administering a fluid bolus challenge or exercise during right heart catheterization particularly if the patient has a resting PCWP between 8 and 15 mm Hg. With regard to the threshold of a mean PAP of 30 mm Hg with exercise, the data to support this as a disease state that is similar to resting PAH are much less robust. The number of pulmonary hemodynamic studies with exercise is small, and a small number of patients were included.<sup>17</sup> Exercise pulmonary hemodynamics have been reported in 218 normal subjects (125 in 1 study of subjects ranging in age

**Exercise Right Heart Catheterization**

**Obtain Baseline hemodynamic Profile**

**Perform arm or leg exercise**

**Goal is 85% age predicted maximal heart rate or elevated PCWP with symptoms**

**Retake measurements during exercise including CO and PA oxygen saturation**

**Fluid Challenge**

**Obtain Baseline hemodynamic Profile**

**Administer 1000 cc 0.9% NaCl iv until completion over 20 minute period or until PCWP exceeds 15 mmHg with symptoms**

**Obtain hemodynamic measurements with every 250 cc volume**

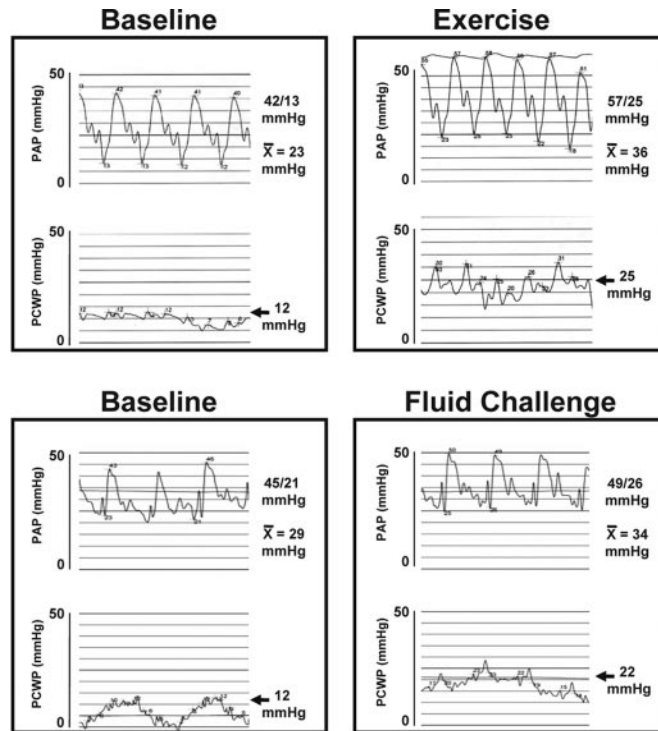


**Figure 2.** Confrontational assessment of cardiopulmonary function by exercise and fluid challenge during right heart catheterization. Top, Johns Hopkins University protocol for exercise right heart catheterization and an example of the results of an exercise challenge in a patient with nonsystolic heart failure (heart failure with preserved ejection fraction, diastolic dysfunction) in which the patient's baseline mean PAP is borderline elevated and PCWP is elevated at 12 mm Hg. With exercise, the PCWP increased significantly to 25 mm Hg with a concomitant increase in mean PAP that resulted from the elevated PCWP. Bottom, The Johns Hopkins University protocol for fluid challenge and an example of data from a patient with pulmonary hypertension and nonsystolic heart failure. At baseline, PAP was elevated (29 mm Hg), as was PCWP (12 mm Hg; note that measures are appropriately measured at end expiration). With fluid challenge, PCWP increased to 22 mm Hg, thus confirming the diagnosis of nonsystolic heart failure. CO indicates cardiac output.

from 14 to 69 years).<sup>17–19</sup> The purpose of exercise is not just to examine PAP in response to exertion. Rather, the benefit of confrontational testing is the observation of the change/increase in PCWP in an effort to diagnose pulmonary venous hypertension or nonsystolic heart failure (diastolic dysfunction; Figure 2). Although protocols for exercise and workload vary from study to study and few subjects have been exercised to maximal workload, the main goal of exercise is to increase heart rate to 85% maximal age-predicted heart rate as is used in cardiology stress testing. Given increased thoracic pressure changes with exercise, particularly in overweight and/or deconditioned patients, it is critical that measurements be made at end expiration to ensure uniformity in interpretation. An increase in PCWP to >15 mm Hg in response to exercise or fluid challenge suggests the presence of pulmonary venous hypertension (Figure 2), a condition with dramatically different management than PAH. Because cardiac output can increase up to 5 times baseline, pulmonary vascular resistance (PVR) normally decreases with exercise (Figure 2).<sup>17,18</sup> Poor prognostic signs in exercise right heart catheterization are the inability of the RV to augment in response to exercise (ie, lack of a significant increase in cardiac output), failure to reduce PVR with exercise, angina, and presyncopal symptoms or frank syncope.

**Novel Hemodynamic Techniques****PA Wave Reflection as a Component of RV Load and Measurement of PA Input Impedance**

Chronic pulmonary hypertension results from an increase in PVR, which is a simple measure of the opposition to the mean component of flow. However, given the low-resistance/high-compliance nature of the pulmonary circulation, the pulsatile component of hydraulic load is also critical to consider. The fact that the mean and the pulsatile components of flow are dependent on different portions of the pulmonary circulation suggests that they could be controlled separately without much overlap. The pulmonary circulation is pulsatile with multiple bifurcations, and wave reflection is an inevitable consequence. When the forward pressure wave from the heart collides with the backward pressure wave that was reflected from the bifurcations, pressure increases and flow decreases. Because the often-used PVR takes only mean flow into account, it does not allow for changes in pulsatility of the pulmonary circuit (Figure 3).<sup>20–23</sup> One must consider the elastic properties of the pulmonary circulation/left atrium and impedance on RV performance rather than the pure resistive properties because the heart could not function if it were not for the elastic properties of pulmonary vasculature. During systole, the pulmonic valve is open at a time when the mitral valve is closed. Thus, if it were not for the elastic properties

**A Measurement of Pulmonary Arterial Input Impedance**

Micromanometer catheter is inserted into the pulmonary artery in close proximity to the pulmonic valve.

Pulmonary artery blood flow can be measured with an intravascular Doppler catheter or with transthoracic echocardiography

Simultaneous measurements of pulmonary arterial pressure and flow are made.

Fourier analysis of pressure and flow data and computation of impedance are made using appropriate software

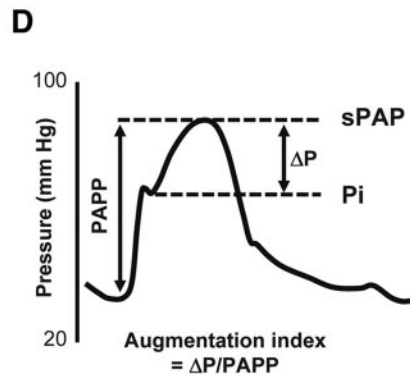
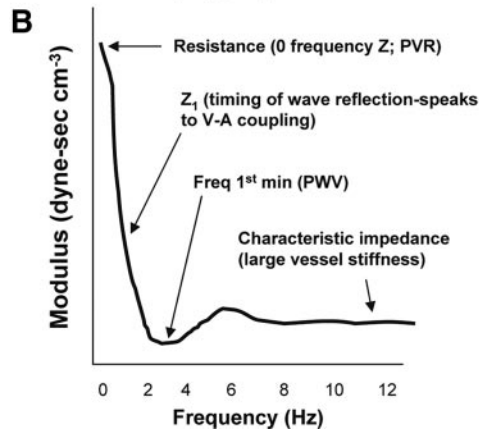
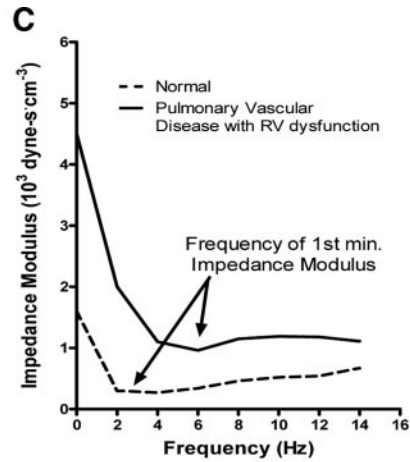


**Figure 3.** Assessment of pulmonary circulation-RV interactions using impedance analysis and augmentation index. A, Outline of technique used to measure simultaneous PAP and flow to compute PA input impedance. B, Schematic highlighting key features of summary impedance spectra. Impedance, the opposition to blood flow by the pulmonary circulation, is frequency dependent on and modulated by heart rate, vessel dimensions, vessel stiffness, and wave reflections.  $Z_0$  is total resistance that does not take into account frequency and represents total PVR. C, Sample impedance spectra from a patient with normal pulmonary circulation (dashed line) showing a baseline  $Z_0$  (PVR) and frequency of first minimal impedance modulus (pulse-wave velocity [PWV]) of  $\approx 2$  to 3 Hz. Solid line shows impedance spectra from a patient with severe pulmonary vascular disease and RV dysfunction in which  $Z_0$  is elevated and there is significant delay in  $Z_1$ , indicating poor RV-pulmonary circulation coupling. In addition, the patient with pulmonary vascular disease displays a significant shift in the frequency of first minimal harmonic and in elevated characteristic impedance, suggesting increased large-vessel stiffness. D, Measurement of augmentation index using PA tracing (time-domain analysis). An increase in augmentation index suggests increased wave reflection in the pulmonary circulation. sPAP indicates systolic pulmonary arterial pressure; Pi, input pressure; PAPP, pulmonary arterial pulse pressure.

of the pulmonary vasculature, the heart could not develop forward flow.<sup>21-23</sup>

**Frequency-Domain Analysis of the Pulmonary Circulation: PA Input Impedance**

The concept of the RV-pulmonary circulation operating as a unit is best demonstrated by the change in hydraulic load that occurs in the setting of PA stiffening and is an early and important component of the vascular remodeling in PAH. As the RV is met with increased hydraulic wave reflection (largely from increased pulmonary stiffness, resulting in decreased pulsatility) in the diseased pulmonary vasculature, its workload is greater to maintain forward flow. Impedance is a measure of the opposition to the pulsatile components of flow. RV afterload is usually considered in terms of PVR. Yet, between one third and one half of the hydraulic power in the main PA is contained in the pulsatile components of flow. Therefore, measurement of arterial input impedance is needed

to obtain a complete description of ventricular afterload. It is also likely that “early” or more severe pulmonary hypertension is missed simply because this contribution to the load on the RV is not accounted for in the mean PAP measurement at the time of right heart catheterization. Research in pulmonary vascular disease has so far focused essentially on the small PAs, which appear to be the main site of resistance. Impedance is dependent primarily on the mechanical properties and the geometry of the proximal PAs. The PA input impedance spectrum is dependent primarily on the first 5 orders of bifurcation from the main PA in decreasing levels of importance and lends credence to the idea that the “total resistance” does not lie solely at the level of arterioles that are  $<250 \mu\text{mol/L}$  in diameter.<sup>21-24</sup> The changes in impedance resulting from large-artery stiffening or remodeling alone can markedly alter the load on the RV. Interestingly, this can occur in the absence of a change in PVR. Moreover, congenital cardiac disease with or without surgical correction (especially

### A Measurement of Right Ventricular Pressure-Volume Relations

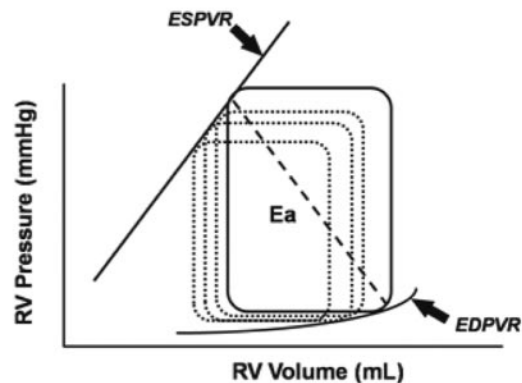
Micromanometer/conductance catheter is inserted into the right ventricle via the right internal jugular vein

Simultaneous measurements of right ventricular pressure and volume are made under steady-state conditions at end-expiration.

ESPVR is made by reducing RV preload using a balloon inflated in the inferior vena cava or forced Valsalva maneuver.

Pressure-volume relationships are computed using specialized software.

C



B



D

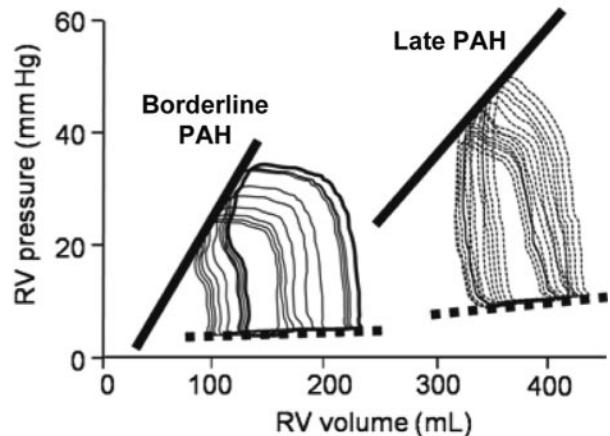


**Figure 4.** RV PV loop relationship analysis in patients with pulmonary vascular disease. A, Outline of technique used to measure simultaneous RV pressure and volume. B, Sketch of placement of conductance catheter (Millar Instruments, Houston, Tex) in the RV to obtain PV data. C, Schematic of basic measures of pressure and volume relationships. The end-systolic PV loop relationship (ESPVR) and end-diastolic PV loop relationships (EDPVR) define the boundaries of the PV loops for a given contractile state of the ventricle. Changing the preload (as shown with dashed lines) or afterload will change the shape and position of the loops, but the end-systolic and end-diastolic points will always fall on the ESPVR and EDPVR. This is the reason why the ESPVR and EDPVR are used as load-independent measures of contractility. The ratio of end-systolic pressure ( $P_{es}$ ) to stroke volume has the dimension of elastance (mm Hg/mL) and is called the arterial elastance ( $E_a$ ) because it is linked to the afterload, which is determined by the arterial system and is represented in the PV loop by the slope of the line that links  $P_{es}$  and end-diastolic volume. D, Representative tracings of RV PV loops in borderline PAH with preserved ESPVR and stroke volume (left) and late PAH with higher RV end-diastolic pressure, end-diastolic volume, and RV end-systolic pressure with a lower stroke volume and decreased contractility (shifted ESPVR to the right).

in repaired tetralogy of Fallot with transannular patch) can significantly increase the pulsatility of the PA waveform. Moreover, with the pulmonic valvular insufficiency that often accompanies congenital disease, there is an increased diastolic volume/load exerted on the RV. With diseases such as scleroderma-related PAH and idiopathic PAH (IPAH), both large-artery and small-artery remodeling occurs, which increases resistance and impedance. However, it is more likely that large-artery involvement (as seen in scleroderma-related PAH or cardiovascular aging) plays a more significant role compared with IPAH in increasing impedance. This abnormal pulsatile load may have detrimental effects on ventricular-vascular coupling by increasing the pulsatile part of ventricular power and thus unfavorably loading the still-ejecting RV.

Several studies have documented the relationship between pulsatile pressure and flow (pulmonary input impedance; Figure 3).<sup>21,23,25–27</sup> The first assessment of pulmonary vascular impedance dates back to 1961, shortly after impedance was first described in the systemic vascular bed.<sup>21,23,28</sup> However, given the previous technical challenges in obtaining impedance spectra, its use has largely been relegated to the laboratory and reported in a few relatively small clinical trials. Only recently have we been able to measure PA input impedance routinely as a result of the ability to measure PA blood flow and PAP simultaneously with high-fidelity catheters at the time of routine right heart catheterization, adding only 5 to 10 minutes to each case.<sup>20,29</sup> These measurements of simultaneous pressure and flow are then used to calculate the

arterial input impedance spectra and have been greatly facilitated by software that can accomplish this task quickly, although the software is not currently commercially available (eg, Matlab-based custom software). This calculation of impedance allows a more accurate quantification of RV hydraulic load from a spectral analysis of pressure and flow waves. The results of this analysis are expressed as an impedance spectrum, consisting of a pressure-to-flow ratio and a phase angle, both of which are expressed as a function of frequency. As shown in Figure 4B, the impedance spectrum includes a measure of total PVR; indexes of wave reflection such as the first minimum of the ratio of pressure and flow moduli or low-frequency phase angle; characteristic impedance ( $Z_c$ ), which corresponds to the ratio of inertance to compliance; and hydraulic load, as evaluated by low-frequency impedance and the amplitude of impedance oscillations. Prior studies have shown that the pulsatile load is also increased in chronic pulmonary hypertension, as suggested by the increased characteristic impedance and enhanced wave reflection that have generally been attributed to decreased PA compliance and complex changes in reflection sites. Moreover, pulmonary vascular impedance has been studied in the pediatric population, in which it was found to predict outcomes better than PVR.<sup>30</sup> Impedance, in combination with compliance and resistance, has been studied with MR technology, which has shown that these techniques may differentiate between types of pulmonary hypertension.<sup>31</sup> Finally, echocardiographic measurements of pulmonary vascular impedance have recently been shown to be feasible.<sup>20</sup> It is hoped that the study of pulmonary vascular impedance will yield important information about the RV response to stress in pulmonary hypertension and may prove to be a more predictive measure of prognosis and response to treatment than current standards.

### Time-Domain Analysis of PA Pressure Waveforms

Although we believe that the measurement of pulmonary vascular impedance may, in the future, become a routine test in patients with PAH, the technology and necessary equipment may currently limit its widespread use outside tertiary care academic centers.<sup>32</sup> Time-domain analysis of pulse pressure and pressure waveform may provide valuable information on pulsatile arterial load and may be a surrogate to the full assessment of RV input impedance (Figure 3).<sup>32</sup> Pulse pressure indicates the amplitude of pulsatile stress. Pulse pressure is determined mainly by both the characteristics of ventricular ejection and arterial compliance; the lower the compliance is, the higher the pulse pressure is. Moreover, pressure waveform analysis performed in the time domain makes it possible to calculate the timing and extent of wave reflection in systemic and pulmonary circulation with measures such as augmentation index (as shown in Figure 3D), which roughly represents reflected wave summation ( $\Delta P$ ) in the pulmonary circuit and normalizes for the PA pulse pressure.<sup>32–40</sup> These values can be obtained easily at the time of right heart catheterization, and future studies will compare both analyses as potential prognostic indicators in patients with pulmonary hypertension and correlate with the previously described concept of capacitance.<sup>41</sup>

### RV Pressure-Volume Loop Relations

The use of pressure-volume (PV) loop analysis as a means of measuring load-independent contractility has largely been restricted to the study of LV hemodynamics and the interaction between the LV and the systemic vasculature.<sup>27,38,42–52</sup> This has been due primarily to geometric differences between the 2 ventricles, the optimal conductance properties required for proper volume measurements, and the belief that it is difficult to obtain consistent data with conductance measurements in the crescent-shaped RV. Indeed, under conditions of normal PAP and RV function, RV PV loop analysis is somewhat complicated given the crescent shape of the normal RV (Figure 1) and the ellipsoid shape of the PV loop obtained under these conditions. However, under conditions of even only modestly increased load, the RV shape changes to one resembling the more spherical LV, allowing measurement of end-systolic elastance and effective arterial elastance, as well as the more accurate measurements of indexes of RV systolic and diastolic function and RV/PA coupling (Figure 4). As shown in Figure 4, the performance of such studies is relatively easy and can be made in the same acquisition time as measurements of impedance spectra with Food and Drug Administration–approved equipment. Because essentially all of the currently used PAH therapies (particularly prostaglandin analogs,<sup>53</sup> phosphodiesterase inhibitors,<sup>4,54–57</sup> and endothelin receptor antagonists<sup>58–60</sup>) and many of the emerging experimental therapies (eg, imatinib) have primary effects on the myocardium (whether positive or negative), a study of the intrinsic contractility of the RV is perhaps the only reliable way to separate the effects of these therapies on the PAs from those on the RV myocardium. In that sense, studies of RV contractility are not only relevant to the clinical management of PAH patients but also critical for the interpretation of the clinical trial data. Moreover, many of the measurements taken with conductance catheterization can be reproduced using measures of RV pressures and cardiac output/stroke volume by right heart catheterization and ventricular volumes as measured by echocardiography, CT, or MRI using standard equations.

## Echocardiography

### Standard Echocardiographic Approaches

#### Estimating Pulmonary Pressures and Resistance

Doppler echocardiography is the most commonly used screening modality for the assessment of RV structure and function, and it allows exclusion of valvular, primary myocardial, and congenital causes of increased right heart pressures. The tricuspid regurgitant jet is generally used to estimate RV systolic pressure via the Bernoulli equation ( $4v^2$ , where  $v$  is the maximum velocity of the tricuspid valve regurgitant jet; Figure 5). An estimated right atrial pressure (based on collapsibility of the inferior vena cava best visualized in the subcostal window<sup>61</sup>) is added to the peak systolic pressure gradient of the tricuspid regurgitant flow to obtain RV systolic pressure (which approximates PA systolic pressure in the absence of pulmonary valve stenosis and RV outflow tract obstruction). Although mean PAP can be estimated by measuring the early diastolic velocity of the

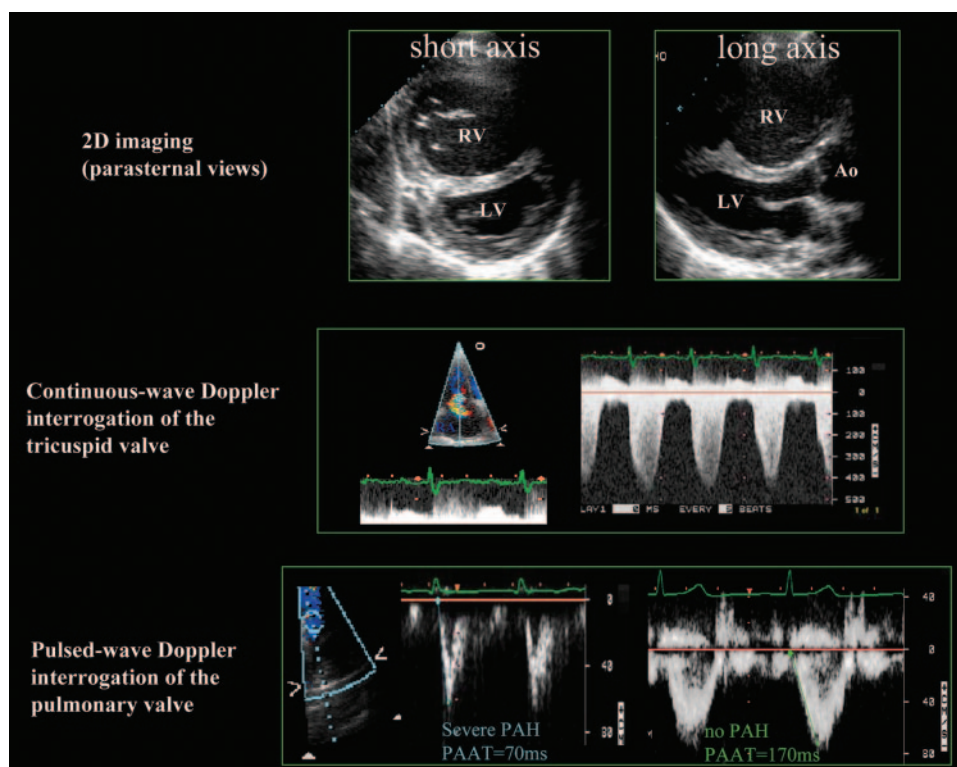


**Figure 5.** Use of echocardiography in assessing pulmonary hypertension. Top, Representative images of echocardiograph 2-dimensional imaging and Doppler assessments in PAH. Note the septum shift toward the LV from RV pressure overload, resulting in a decrease in LV volume and perhaps a secondary increase in LV filling pressures. Middle, The standard tricuspid regurgitation velocity method currently used to estimate systolic PAP (see text) using continuous-wave Doppler. Bottom, Pulsed-wave Doppler interrogation of the main PA to measure PAAT (the time from the start of the envelope to its peak) in patients with severe PAH (left) and no PAH (right). In pulmonary hypertension, the peak velocity of the Doppler envelope decreases and the time to peak velocity (measured from the onset of flow) or PAAT shortens. In severe pulmonary hypertension, there may be “notching” or early systolic deceleration, which, like the premature partial closure of the pulmonic valve on M mode, reflects reflection of velocity waves and cancellation by reverse flow. EDV indicates end-diastolic volume; ESV, end-systolic volume; EF, ejection fraction; TAPSE, tricuspid annular plane systolic excursion; RA, right atrium; and RVD, RV dimension.

pulmonary insufficiency jet, the correlation with invasive measures is weak because of difficulty in accurately visualizing the velocity regurgitant profile at the pulmonary valve. More recently, formulas for estimating mean PAP from the RV systolic pressure have been developed.<sup>62,63</sup> In addition, Doppler echocardiography allows noninvasive estimation of PVR, measured as the ratio of the tricuspid regurgitant velocity to the velocity-time interval of the RV outflow tract. The ratio of tricuspid regurgitant velocity to the velocity-time interval of the RV outflow tract has recently been shown to predict mortality and adverse cardiovascular events in patients with stable coronary artery disease,<sup>64</sup> but its usefulness in patients with pulmonary vascular disease<sup>65</sup> remains to be determined.

Initial studies by Berger et al<sup>66</sup> and Currie et al<sup>67</sup> demonstrated good correlation between echocardiographic estimates and directly measured pressures. However, there are conflicting data as to the strength of this correlation between RV systolic pressure estimated by Doppler echocardiography and mean PAP measured via right heart catheterization. When RV and PAPs are estimated via echocardiography, they more often are higher than the pressures measured directly by catheterization, and although it is clear that Doppler echocar-

diography cannot be recommended at this time for use as the gold standard for diagnosis of pulmonary hypertension, it remains an excellent screening modality.<sup>66,68,69</sup> Aside from a significant increase in RV systolic pressure, patients with more severe pulmonary hypertension classically present with right atrial dilatation, RV hypertrophy and dilatation, evidence of RV remodeling (thickening of the “moderator band”), and systolic flattening of the interventricular septum with D-shape deformity suggesting pressure overload (Figure 5). The presence of pericardial effusion has been correlated with poor survival in IPAH<sup>69,70</sup> and in patients with scleroderma-related PAH.<sup>71</sup>

Exercise echocardiography has been suggested as a reliable means to detect pathological increases in PAPs. One example has been its use in patients at risk for pulmonary hypertension.<sup>72</sup> However, this test has not been standardized, and interpretation of changes with exercise has to be considered with caution, particularly because age- and gender-related variations have not been fully elucidated. It is noteworthy that significant elevations of PAP can occur in well-trained athletes at peak workloads<sup>73</sup> or in patients with impaired LV filling.<sup>74</sup> The use of exercise echocardiography is not specifically recommended at this time to assess patients with PAH.

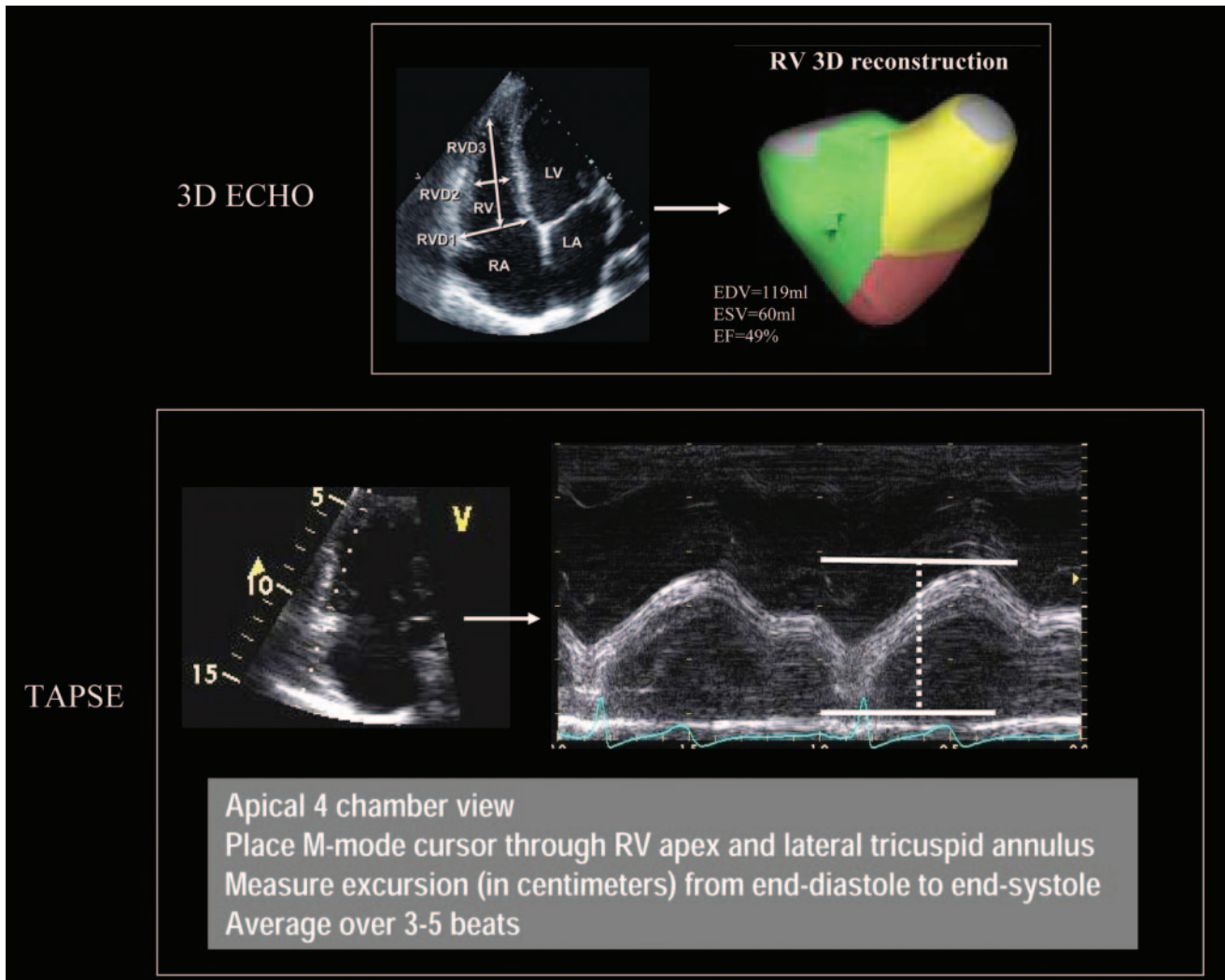


**Figure 6.** Top, Example of 3D echocardiography in which multiple views of the RV are reconstructed to provide a 3D volumetric image for assessment of RV volumes and function (Courtesy Kirk Spencer, MD, and Lissa Sugeng, MD, MPH, University of Chicago). Bottom, Representative M-mode recording through the lateral tricuspid valve annulus for the purpose of measuring the tricuspid annular plane systolic excursion. Excursion is measured from end diastole to end systole as shown on right. Ao indicates aorta.

## Novel Uses of Echocardiography

### Estimating RV Function

RV dysfunction and hypertrophy may be difficult to quantify on echocardiography<sup>75</sup> because of the complex geometry and poor RV endocardial definition, the characteristic mode of myocardial contraction related to muscle fiber orientation (compared with the LV), and operator and acoustic window differences that determine image quality. However, when present, these findings can provide important information about cardiac effects of chronic pressure overload. Three-dimensional (3D) echocardiography can give accurate estimates of RV ejection fraction, structure, and function; however, this technique is not currently widely available (Figure 6).<sup>76</sup> Great attention has been paid to alternative measures of RV function. The Tei index yields a computed value that combines Doppler-derived RV systolic and diastolic function to assess RV function quantitatively.<sup>77</sup> Indexed right atrial area, the degree of septal shift in diastole, and a high Doppler RV performance index have been associated with poor

outcomes.<sup>70</sup> These measurements, although not routinely obtained in the standard echocardiogram, can be made in clinical practice. More recent studies have focused on the value of echocardiography in assessing RV function by various techniques, including 2-dimensional strain, tissue Doppler echocardiography, tridimensional echocardiography, or the speckle tracking method.<sup>78,79</sup> Systolic and diastolic tissue Doppler imaging–derived velocity profiles of the RV free wall and the lateral tricuspid annulus may also help detect early RV dysfunction.<sup>80,81</sup> For instance, quantification of RV function can be estimated by ultrasonic strain-rate imaging. The local rate of the wall deformation (strain rate) and the amount of deformation (strain) can be measured by processing regional myocardial velocity data. Strong correlations have been reported between apical strain and invasively measured mean PA and PVR. Similarly, derivation of regional RV isovolumetric relaxation time (defined as the interval between pulmonary valve closure and tricuspid valve opening) from tissue velocity recordings of RV myocardial

wall motion (at the tricuspid annulus along the long axis) correlates strongly with invasively measured PA systolic pressure when corrected for heart rate. However, there is loss of correlation between PA systolic pressure and corrected isovolumetric relaxation time in the presence of significant RV dysfunction. Therefore, corrected isovolumetric relaxation time can be considered a simple and reproducible measurement of PA systolic pressure (and an alternative to tricuspid regurgitation–derived PA systolic pressure when tricuspid regurgitation cannot be recorded for technical reasons); however, results should be interpreted with caution when RV function is depressed.

More recently, measurement of the **tricuspid annular plane systolic excursion** as a marker of RV ejection fraction has been shown to be an important prognostic marker in PAH.<sup>82</sup> This measurement is based on the observation that the stroke volume of the RV is largely related to shortening of the longitudinal axis (thus drawing the tricuspid annular plane toward the cardiac apex) rather than reduction in the cavity diameter, as is the case for the LV. This measurement can be made on standard M-mode or 2-dimensional echocardiography and is therefore widely available (Figure 5). Aside from predicting survival (which was poor for a tricuspid annular plane systolic excursion value <1.8 cm), this simple measurement accurately reflects RV remodeling, RV-LV disproportion (RV/LV diastolic area), and load (PVR).<sup>82</sup> Thus, given the wide availability of M-mode and dimensional echocardiography, tricuspid annular plane systolic excursion may prove to be the most useful marker of RV function and structure (eg, remodeling) that is available to the broadest population of practitioners. Finally, 3D echocardiography might provide better insight into RV and LV dimension and function by obviating geometric assumptions (Figure 6).

In the future, **greater attention may be paid to RV diastolic function**. This can be assessed in much the **same way as the LV with E/A and E'/A' analysis**.<sup>35,83</sup> Moreover, diastolic forward flow in the RV outflow tract may serve as a marker of RV diastolic function.<sup>83–85</sup> More recently, the improvement of PAH therapy on RV diastolic function has been noted.<sup>83</sup>

### Pulsed Doppler

Pulsed Doppler measurement of PA flow velocity in the main PA is an extremely useful qualitative and quantitative technique for measuring PAP and, unlike estimates based on tricuspid regurgitation velocity, is available in virtually all patients. In pulmonary hypertension, the peak velocity of the Doppler envelope decreases, and the time to peak velocity (measured from the onset of flow) or PA acceleration time (PAAT) shortens. In severe pulmonary hypertension, there may be “notching” or early systolic deceleration, which, like the premature partial closure of the pulmonic valve on M-mode echocardiography, represents reflection of velocity waves and cancellation by reverse flow. This is due to the noncompliant nature of the distal vascular bed in pulmonary vascular disease. The normal PA flow velocity is  $81 \pm 17$  cm/s and occurs with a PAAT of  $121 \pm 27$  seconds.<sup>86</sup> A typical Doppler signal in patients with pulmonary hypertension is often triangular rather than the normal broad shield shape

seen in normotensive patients, and the PAAT is shortened (Figure 5).<sup>87</sup> Although there is a fair correlation between acceleration time and PA systolic pressure, Dabestani et al<sup>88</sup> found a better correlation between PAAT and mean PAP, a more physiological measurement. They used a regression equation to develop the following formula predictive of mean PAP:  $\text{mean PAP} = 79 + 0.45 \times \text{PAAT}$ . This relationship has been confirmed, albeit with modified regression formulas.<sup>88</sup> This technique is somewhat dependent on heart rate but correlates well with mean PAP in patients with heart rates between 60 and 100 bpm.

In summary, echocardiography can provide anatomic and functional assessments of both the RV and the pulmonary circulation. Therefore, it is a powerful tool in the assessment of the RV-PA unit, particularly in that novel applications like 3D echocardiography, tricuspid annular plane systolic excursion, and PAAT are used more frequently and are validated in large cohorts and clinical trials.

### Cardiac MR

MRI and MR angiography (MRA) are techniques that can, noninvasively and in a single setting, study the RV-PA unit and provide multiple data ranging from structure (RV volume, mass, pulmonary angiography) to function (RV function, pulmonary blood flow [PBF]/perfusion) to molecular imaging. All of the described studies can be performed in standard clinical 1.5-T magnets and can be completed without or with a small amount of gadolinium contrast injected through a peripheral vein. More important, they can be completed within a short period of time (ie, **<1 hour**), providing a comprehensive assessment in a **“single-stop shop”** manner.

### Standard MRI Approaches

#### RV Mass and Volume

There have been major advances in MRI techniques in the last several years with ECG gating and respiratory suppression, diminishing imaging artifacts and allowing computations of RV volumes. The **complex 3D structure of the RV** can be directly **studied with MRI** to measure RV volume and mass<sup>89,90</sup> without the need for computational assumptions; values for RV mass and volume in normal cohorts also have been reported.<sup>91</sup>

Conventional (gradient-recalled echocardiography) or newer (steady-state free precession pulse) sequences can be used to create cine images of a complete cardiac cycle. In stacks of contiguous 5- to 10-mm slices, endocardial and epicardial contours can be drawn in end systole and end diastole (Figure 7).<sup>92,93</sup> The sum of the individual slice volumes will give the end-systolic (RVESD) and end-diastolic (RVEDV) volumes, from which RV ejection fraction (RVEF) can be calculated:  $\text{RVEF} = (\text{RVEDV} - \text{RVESV}) / \text{RVEDV}$ . RV mass can be calculated by multiplying RV volume by the myocardium specific gravity ( $1.05 \text{ g/cm}^3$ ). The anatomy of the RV is more complex than the LV, and moderator bands can vary in presence and size; some might include them in the tracing of the RV endocardial contour, whereas others might not. This results in somewhat lower interstudy reproducibility in the RV compared with the LV,

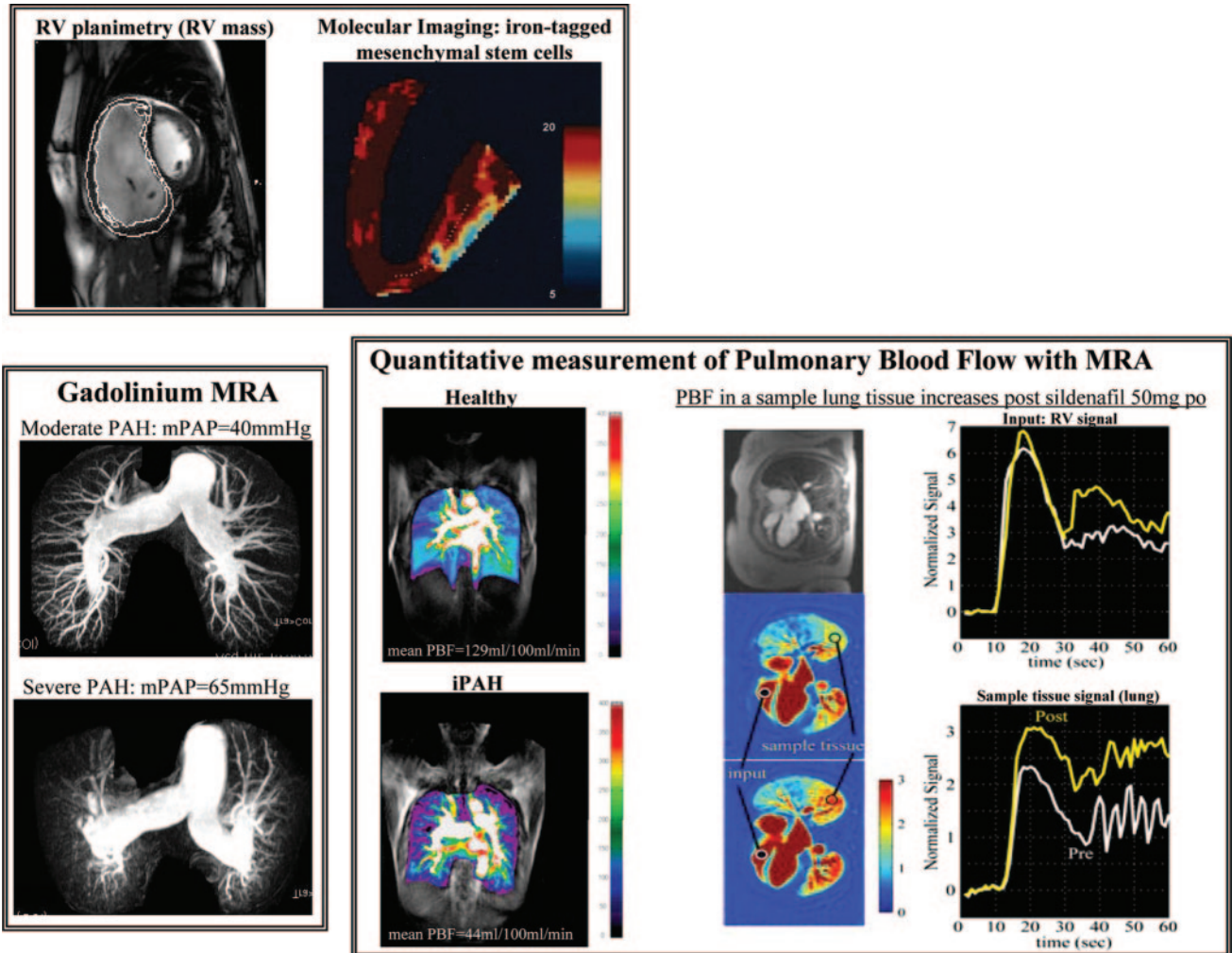


**Figure 7.** MRI and the RV-PA unit. Top left, Standard MRI techniques can be used to trace the endocardium and epicardium of the RV and to calculate RV volumes in systole and diastole, as well as RV mass, as discussed in text. Top right, Iron tagging of cells used in cell-based therapies can be used to track the homing of these cells in both the pulmonary circulation and the RV. In this example from Hill et al,<sup>92</sup> the homing of mesenchymal cells in an infarct area of the LV is shown. Used with permission. Copyright © 2003 Lippincott Williams & Wilkins). Bottom left, Gadolinium injection in a peripheral vein shows a much worse obliterative remodeling, resulting in less opacified vessels, in a patient with a severe compared with moderate PAH, correlating with invasively measured mean PAPs (mPAP). Bottom right, On the left, Ohno and colleagues<sup>93</sup> show mean PBF measured, after a small gadolinium infusion, in a healthy subject vs a patient with severe iPAH, showing the quantitative nature of this technique (see text). Used with permission. Copyright © 2007 American Roentgen Ray Society. On the right, a similar technique developed at the University of Alberta (see text) showed that the decrease in PBF in a patient with iPAH after 50 mg sildenafil PO was similar to the ≈35% decrease in PVR measured during catheterization. These data suggest that such techniques can be used to generate quantitative end points in clinical trials in the future.

but this is overall very high and definitely better than echocardiography,<sup>94,95</sup> making MRI the gold standard for the study of RV size and function. The published data for interstudy reproducibility in MRI-studied RV size can be useful in calculations of sample sizes in clinical trials. Although the RV ejection fraction and calculation of stroke volumes can be complicated by the presence of significant tricuspid regurgitation (similar to mitral regurgitation and the LV), the calculation of RV volumes is direct and not affected by other factors.

RV hypertrophy is mostly an adaptive or compensated state in response to the increased RV afterload (Figure 1). During that stage, RV mass correlates well with PAP.<sup>96,97</sup> Beyond that stage, RV enlargement is associated with a decrease in RV contractility, further decreases in cardiac

output, worsening right heart failure, and death. Therefore, it is not surprising that in a prospective study of 64 PAH patients followed up for 32 months, RV volume at diagnosis was a strong predictor of mortality, stronger than RV mass.<sup>98</sup> Further RV dilatation at follow-up was an even stronger predictor of survival.<sup>98</sup>

Studies are now reporting RV mass changes in response to PAH therapies, showing feasibility in including RV mass/volume as end points in clinical trials. For example, in a small study, RV mass decreased in response to 3 months of sildenafil therapy.<sup>99</sup> In another blinded randomized study, RV mass decreased in response to sildenafil but not in response to bosentan therapy, despite similar decreases in the PAPs.<sup>5</sup> The inclusion of RV mass in this last study suggested the potential for direct effects of sildenafil on the RV, a possibility that

could not have been predicted by hemodynamic values alone. This possibility was later confirmed by studies showing a significant increase in phosphodiesterase type 5 expression (the target enzyme of sildenafil) in the hypertrophied (but not the normal) RV myocardium.<sup>4</sup>

In summary, RV mass and volumes can be easily acquired, do not require sophisticated software or specific operator skills, and can provide valuable quantitative data. Captured in large databases, such data could easily be validated in larger cohorts and finally included as primary end points in large multicenter clinical trials.

### **Pulmonary Angiography**

The loss of perfusion in the distal PAs, resulting from proximal obliterative remodeling and microvessel loss, is recognized both in animal studies and in human PAH, as reflected by the classic sign of pulmonary vascular “pruning” in pulmonary angiography. Loss of peripheral vascularity and branching pattern in the pulmonary vascular tree provides a direct visual assessment of the degree of vascular remodeling, and its regression may reflect response to experimental therapies. Through MRA, a detailed 3D pulmonary angiogram can be obtained with injection of gadolinium in a peripheral vein (Figure 7). Although the quantification of remodeling by angiography has to be developed and validated in the assessment of PAH, MRA can offer additional and clinically relevant information. For example, it can easily detect filling defects that would suggest pulmonary thrombi. Because exclusion of thrombi is an essential part of the workup in PAH and usually requires a CT scan with contrast and a V/Q scan, MRA performed as part of a comprehensive study in a single setting might be an efficient and potentially cheaper alternative.

## **Novel Uses of MRI in Pulmonary Hypertension**

### **Pulmonary Vascular Perfusion**

Early studies using the phase-contrast technique and velocity-encoded MRI showed the feasibility of estimating right-side hemodynamics,<sup>100,101</sup> but the ease of Doppler echocardiography has limited the enthusiasm of proceeding with large-scale validation studies. Furthermore, these parameters are dependent on many factors beyond the pulmonary microcirculation; eg, pulmonary flow increases in anemia or in liver failure, resulting in increased systolic PAPs without a true increase in PVR. In addition, because RV function deteriorates and is unable to support forward flow, the PAP might drop, giving a false sense of improvement. Thus, the measurement of PAP is not necessarily a sensitive index of the condition of the pulmonary vasculature. The high capacitance of the pulmonary circulation results in a rise in PAP only after a very large percentage of the pulmonary vasculature has been compromised. It is surprising that despite the progress in the imaging of tissue perfusion in organs like the heart and brain, there are currently no widely used clinical tests for pulmonary tissue perfusion. This is unfortunate because whether there is microvessel loss early in the disease or proliferative obliterative remodeling in more proximal vessels later on in the development of PAH,<sup>102,103</sup> there is loss of blood flow and tissue perfusion. The aim of all current and future therapies

for PAH is to increase tissue perfusion, whether by regenerative approaches early or by antiremodeling strategies later.<sup>1,102</sup> There is indeed a great need for methods that can assess the pulmonary circulation directly and quantitatively.

Recent advances in MRA have made it possible to calculate regional quantitative perfusion parameters in the lung on the basis of 3D contrast-enhanced dynamic MR perfusion and principles of the indicator dilution theory.<sup>104–108</sup> After validation in animal models, these techniques have now been applied in humans<sup>108,109</sup> (Figure 7). Using standard 1.5-T machines, pulses, and a single gadolinium injection as low as 2 to 5 cm<sup>3</sup>,<sup>93</sup> we can directly measure PBF in different regions of the lung. In a recent study measuring PBF with this technique in normal volunteers and patients with IPAH who underwent both MRA and cardiac catheterization, the PBF in the 2 groups differed significantly (129.6±14.6 versus 70.9±10 mL · 100 mL<sup>-1</sup> · min<sup>-1</sup>, respectively; n=14 per group; *P*<0.0001).<sup>110</sup> Moreover, PBF had a strong negative correlation with PVR and moderate negative correlation with mean PAP, as would be expected.<sup>93</sup>

In Figure 7, regional quantitative pulmonary perfusion is shown in a healthy man. The mean PBF in the slice shown was 126 mL · 100 mL<sup>-1</sup> · min<sup>-1</sup>. In contrast, in a patient with IPAH, there is a significant decrease in the mean PBF to 44 mL · 100 mL<sup>-1</sup> · min<sup>-1</sup>.<sup>93</sup> In another example shown in Figure 7, a patient with IPAH was studied at the University of Alberta with a similar technique, and the increase in PBF after a single dose of 50 mg sildenafil given orally is shown. Although the contrast agent arterial input function measured in the RV is similar before and after, reflecting consistent venous injections between studies, the contrast delivery in a specific region of the lung increased significantly after sildenafil, reflecting increased tissue perfusion. Such an increase also can be expressed as the area under the curve, as shown, and can be used to track the progress of this patient with time. The same patient showed a similar increase in PVR with sildenafil during catheterization. In the example shown, the images were obtained without a breath hold using respiratory variation suppression protocols, which is a significant advantage because patients with severe PAH often have difficulties with breath holding (Figure 7; courtesy of Drs I. Patterson and R. Thompson, University of Alberta). It is obvious that such a direct and quantitative measurement would be very desirable in the clinical assessment of PAH patients in response to therapies and would be a valuable end point in clinical trials with regenerative and antiremodeling therapies.

Such techniques have potential limitations because many assumptions are made in the equations and modeling of the indicator dilution theory. For example, the blood volume is not equal to the distribution volume of gadolinium because the latter extravasates into the interstitium and lung permeability may vary. It is important to emphasize that the value of measuring PBF with MRA does not lie in measuring the true PBF but rather assessing the “change” in the signal that occurs with disease progression or in response to therapy.

### **RV-PA Interactions**

The more complex hemodynamic studies discussed earlier on RV contractility and RV-PA coupling can also be performed

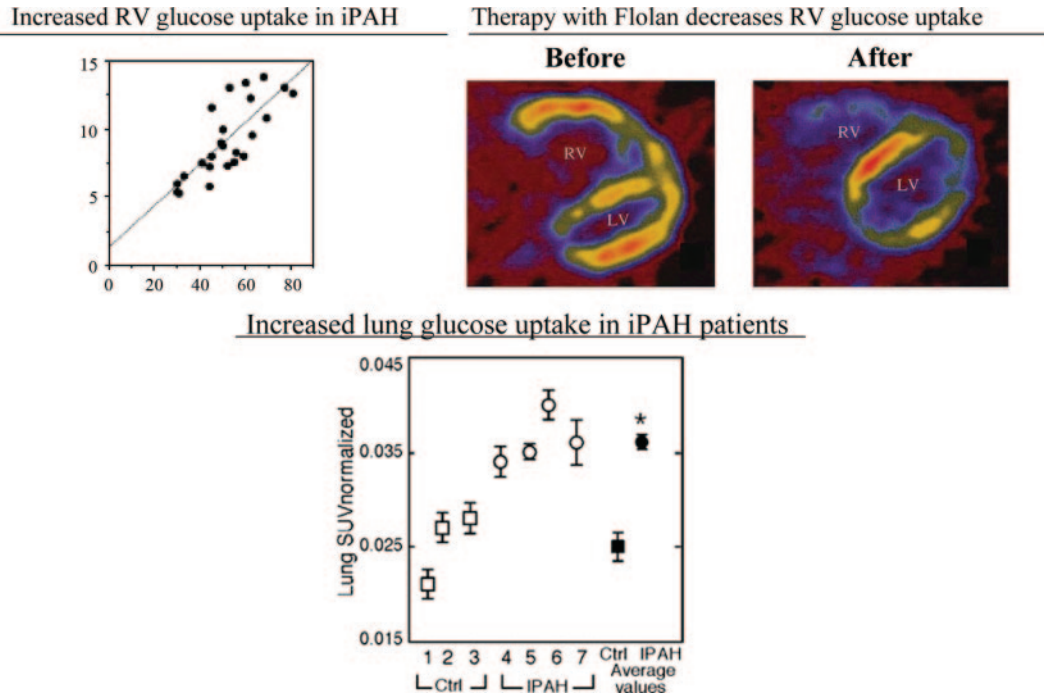


**Figure 8.** PET and the RV-PA unit. Standard FDG-PET imaging can be used to measure RV and pulmonary microcirculation metabolism. Top left, Increased RV FDG glucose uptake (y axis) correlates with mean PAP in a cohort of patients with IPAH (see text). More important, Oikawa and colleagues<sup>125</sup> have shown that effective therapy with Flolan results in a decrease in RV FDG uptake, compatible with a decrease in RV glycolysis, indicating an improvement in RV performance (top right). Reprinted with permission. © 2005 Elsevier. Because RV ejection fraction measurement can be limited by a number of parameters, including tricuspid regurgitation, RV metabolism might prove to be a more sensitive way to follow RV function in PAH patients. Bottom, At the same time as RV imaging, FDG uptake can be followed in the pulmonary microcirculation, where an increase in FDG uptake (resulting from an increase in glycolysis) is associated with a proliferative and antiapoptotic state (see text). In this small cohort of PAH patients and normal control subjects, Xu et al<sup>119</sup> show that FDG uptake in the lung parenchyma is much higher in the PAH patients vs normal subjects. Reprinted with permission. Copyright © 2007 National Academy of Sciences USA.

with MRI, as early evidence indicates. RV contractility can be studied using several parameters, including MRI-derived PV loops.<sup>111</sup> Large PA stiffness can also be studied with MRI, as can RV diastolic dysfunction,<sup>83</sup> a potentially early finding in PAH.

**Molecular Imaging**

Systemically delivered proapoptotic or regenerative cell-based therapies can obviously affect the RV and the pulmonary circulation. Tracking the molecular response in both the PAs and the RV will be important for the assessment of such experimental therapies. Apoptosis imaging is used in oncology to assess the early and late effects of proapoptotic chemotherapies in tumors. A large number of emerging therapies in PAH are proapoptotic, but induction of apoptosis in the myocardium can be detrimental. For example, the anticancer agent imatinib, which has shown promise as an antiremodeling agent in PAH,<sup>6</sup> might cause apoptosis in the heart, perhaps explaining its documented myocardial toxicity.<sup>7</sup> In vivo induction of apoptosis can be tracked, localized, and quantified with annexin V imaging.<sup>112,113</sup> Annexin V is expressed on the cellular surface of cells undergoing early apoptosis, and binding of annexin to superparamagnetic iron particles allows MRI-based detection of apoptosis in vivo.<sup>114</sup> Therefore, a single study can assess the effects on both the PA and the RV. Furthermore, iron-tagged cells can be tracked and their homing and retention quantified, as illustrated by

the presence of mesenchymal stem cells in an ischemic LV<sup>92</sup> (Figure 7, top right).

**PET Imaging**

Among the many functions that can be imaged with PET imaging is glucose uptake. Increased glucose uptake is usually associated with a glycolytic phenotype. A switch from the mitochondria-based glucose oxidation to the cytoplasm-based glycolysis, even in the absence of hypoxia, is recognized in many disease states characterized by increased proliferation and suppressed apoptosis.<sup>115</sup> This is well described in cancer<sup>116,117</sup> and has been suggested more recently in PAH vascular remodeling.<sup>118,119</sup> In addition, a switch to glycolysis (from fatty acid oxidation) characterizes cardiac hypertrophy<sup>120,121</sup>; the hypertrophied RV myocardial cells have hyperpolarized mitochondria (compared with the normal RV cardiomyocytes),<sup>103</sup> similar to the hyperpolarized mitochondria of cancer cells.<sup>122</sup> Similarly, PA smooth muscle cells have hyperpolarized mitochondria compared with normal PA smooth muscle cells.<sup>118</sup> In that sense, glycolysis (and thus increased glucose uptake) characterizes both the pulmonary circulation (proliferating PA smooth muscle cells<sup>118</sup> and PA endothelial cells<sup>119</sup>) and RV hypertrophy<sup>123</sup> in PAH (for further discussion, see Reference 1, another article in this series). It is thus possible that the degree of glucose uptake (measured by the standardized uptake value of <sup>18</sup>F-fluorodeoxy-glucose [FDG] with PET) might correlate

with both the degree of vascular remodeling and RV function in PAH and in response to therapy in a manner similar to cancer.<sup>124</sup> Preliminary data in animals and more recently in humans support this possibility. In 24 patients with PAH, FDG-PET showed increased glucose uptake in the RV free wall corrected for the increase in myocardial volume; the standardized uptake value correlated to mean PAP, PVR, and right atrial pressure (Figure 8).<sup>125</sup> More important, after 3 months of therapy with epoprostenol, the standardized uptake value decreased significantly in the responders but not in nonresponders (Figure 8, top right).<sup>125</sup> In another cohort of 4 PAH patients versus 3 healthy control subjects, FDG-PET showed an increase in the glucose uptake in the lung tissue (a highly vascular tissue reflecting metabolism in the pulmonary microvessels) normalized for lung tissue density<sup>119</sup> (Figure 8, bottom).

Thus, imaging of both the RV and the lungs in the same noninvasive setting and in a quantitative manner such as with MRI and echocardiography might be useful in the study of the RV-PA unit, particularly in response to therapy. If validated in larger cohorts, FDG-PET-measured glucose uptake might be considered an end point in PAH clinical trials. Furthermore, similar to MRI, the new hybrid PET-64-slice CT systems might allow simultaneous acquisition of functional (PET) and high-fidelity anatomic (CT) data in both the RV and pulmonary vessels.

### Acknowledgments

Drs Champion, Hassoun, and Michelakis are fellows of the Pulmonary Vascular Research Institute. Drs Champion and Michelakis are fellows of the American Heart Association.

### Sources of Funding

This work was supported, in part, by the Bernard A. and Rebecca S. Bernard Foundation, a scientist development grant from the American Heart Association, the W.W. Smith Foundation (to Dr Champion), and National Institutes of Health P50 HL084946 (to Drs Champion and Hassoun). Dr Michelakis is supported by the Canadian Institutes for Health Research, the Alberta Heritage Foundation for Medical Research, the Alberta Heart and Stroke Foundation, and the Canada Research Chairs program.

### Disclosures

None.

### References

1. Michelakis ED, Wilkins M, Rabinovitch M. Emerging concepts and translational priorities in pulmonary arterial hypertension. *Circulation*. 2008;118:1486–1495.
2. Voelkel NF, Quaipe RA, Leinwand LA, Barst RJ, McGoon MD, Meldrum DR, Dupuis J, Long CS, Rubin LJ, Smart FW, Suzuki YJ, Gladwin M, Denholm EM, Gail DB. Right ventricular function and failure: report of a National Heart, Lung, and Blood Institute Working Group on Cellular and Molecular Mechanisms of Right Heart Failure. *Circulation*. 2006;114:1883–1891.
3. Ghofrani A, Wilkins MW, Rich S. Uncertainties in the diagnosis and treatment of pulmonary arterial hypertension. *Circulation*. 2008;118:1195–1201.
4. Nagendran JAS, Gurtu V, Webster L, Ross DB, Rebeyka IM, Michelakis ED. Phosphodiesterase type 5 is highly expressed in the hypertrophied human right ventricle: direct implications for patients with pulmonary hypertension. *Circulation*. 2006;114(suppl):II-667. Abstract.
5. Wilkins MR, Paul GA, Strange JW, Tunariu N, Gin-Sing W, Banya WA, Westwood MA, Stefanidis A, Ng LL, Pennell DJ, Mohiaddin RH, Nihoyannopoulos P, Gibbs JS. Sildenafil Versus Endothelin Receptor

- Antagonist for Pulmonary Hypertension (SERAPH) study. *Am J Respir Crit Care Med*. 2005;171:1292–1297.
6. Ghofrani HA, Seeger W, Grimminger F. Imatinib for the treatment of pulmonary arterial hypertension. *N Engl J Med*. 2005;353:1412–1413.
  7. Kerkela R, Grazette L, Yacobi R, Iliescu C, Patten R, Beahm C, Walters B, Shevtsov S, Pesant S, Clubb FJ, Rosenzweig A, Salomon RN, Van Etten RA, Alroy J, Durand JB, Force T. Cardiotoxicity of the cancer therapeutic agent imatinib mesylate. *Nat Med*. 2006;12:908–916.
  8. D'Alonzo GE, Barst RJ, Ayres SM, Bergofsky EH, Brundage BH, Detre KM, Fishman AP, Goldring RM, Groves BM, Kernis JT, Levy PS, Pietra GG, Reid LM, Reeves JT, Rich S, Vreim CE, Williams GW, Wu M. Survival in patients with primary pulmonary hypertension: results from a national prospective registry. *Ann Intern Med*. 1991;115:343–349.
  9. Hoepfer MM, Lee SH, Voswinckel R, Palazzini M, Jais X, Marinelli A, Barst RJ, Ghofrani HA, Jing ZC, Opitz C, Seyfarth HJ, Halank M, McLaughlin V, Oudiz RJ, Ewert R, Wilkens H, Kluge S, Bremer HC, Baroke E, Rubin LJ. Complications of right heart catheterization procedures in patients with pulmonary hypertension in experienced centers. *J Am Coll Cardiol*. 2006;48:2546–2552.
  10. Grossman W, Barry W. Cardiac Catheterization. In: Braunwald E, ed. *Heart Disease: A Textbook of Cardiovascular Medicine*. Philadelphia, Pa: WB Saunders; 1988:247–252.
  11. Grossman WBE. *Pulmonary Hypertension*. 3rd ed. Philadelphia, Pa: Saunders; 1988.
  12. Barst RJ, McGoon M, Torbicki A, Sitbon O, Krowka MJ, Olschewski H, Gaine S. Diagnosis and differential assessment of pulmonary arterial hypertension. *J Am Coll Cardiol*. 2004;43:40S–47S.
  13. Gaine SP, Rubin LJ. Primary pulmonary hypertension. *Lancet*. 1998;352:719–725.
  14. Libby P, Bonow RO, Mann DL, Zipes DP. Cardiac catheterization. In: Braunwald E, ed. *Braunwald's Heart Disease: A Textbook of Cardiovascular Medicine*. 8th ed. Philadelphia, Pa: Saunders Elsevier; 2007:449.
  15. Hemnes AR, Champion HC. Right heart function and haemodynamics in pulmonary hypertension. *Int J Clin Pract Suppl*. 2008;11–19.
  16. Badesch DB, Abman SH, Simonneau G, Rubin LJ, McLaughlin VV. Medical therapy for pulmonary arterial hypertension: updated ACCP evidence-based clinical practice guidelines. *Chest*. 2007;131:1917–1928.
  17. Reeves JT, Dempsey JA, Grover RF. Pulmonary circulation during exercise. In: Weir EK, Reeves JT, eds. *Pulmonary Vascular Physiology and Pathophysiology*. 1st ed. New York, NY: Marcel Dekker, Inc; 1989:107–135.
  18. Brower R, Permutt S. Exercise and the pulmonary circulation. In: Whipp BJ, Wasserman K, eds. *Exercise: Pulmonary Physiology and Pathophysiology in Lung Biology in Health and Disease*. New York, NY: Marcel Dekker, Inc; 1991;52:201–221.
  19. Ehrsam RE, Perruchoud A, Oberholzer M, Burkart F, Herzog H. Influence of age on pulmonary haemodynamics at rest and during supine exercise. *Clin Sci (Lond)*. 1983;65:653–660.
  20. Huez S, Brimiouille S, Naeije R, Vachiery JL. Feasibility of routine pulmonary arterial impedance measurements in pulmonary hypertension. *Chest*. 2004;125:2121–2128.
  21. Kussmaul WG, Noordergraaf A, Laskey WK. Right ventricular-pulmonary arterial interactions. *Ann Biomed Eng*. 1992;20:63–80.
  22. Parmley WW, Tyberg JV, Glantz SA. Cardiac dynamics. *Annu Rev Physiol*. 1977;39:277–299.
  23. Piene H. Pulmonary arterial impedance and right ventricular function. *Physiol Rev*. 1986;66:606–652.
  24. Hess W. Effects of amrinone on the right side of the heart. *J Cardiothorac Anesth*. 1989;3:38–44.
  25. Jalonen J. Invasive haemodynamic monitoring: concepts and practical approaches. *Ann Med*. 1997;29:313–318.
  26. Morpurgo M, Jezek V, Ostadal B. Pulmonary input impedance or pulmonary vascular resistance? *Monaldi Arch Chest Dis*. 1995;50:282–285.
  27. O'Rourke MF. Vascular impedance in studies of arterial and cardiac function. *Physiol Rev*. 1982;62:570–623.
  28. Robotham JL. Cardiovascular disturbances in chronic respiratory insufficiency. *Am J Cardiol*. 1981;47:941–949.
  29. Lankhaar JW, Westerhof N, Faes TJ, Gan CT, Marques KM, Boonstra A, van den Berg FG, Postmus PE, Vonk-Noordegraaf A. Pulmonary vascular resistance and compliance stay inversely related during treatment of pulmonary hypertension. *Eur Heart J*. 2008;29:1688–1695.

30. Hunter KS, Lee PF, Lanning CJ, Ivy DD, Kirby KS, Claussen LR, Chan KC, Shandas R. Pulmonary vascular input impedance is a combined measure of pulmonary vascular resistance and stiffness and predicts clinical outcomes better than pulmonary vascular resistance alone in pediatric patients with pulmonary hypertension. *Am Heart J*. 2008;155:166–174.
31. Lankhaar JW, Westerhof N, Faes TJ, Marques KM, Marcus JT, Postmus PE, Vonk-Noordegraaf A. Quantification of right ventricular afterload in patients with and without pulmonary hypertension. *Am J Physiol Heart Circ Physiol*. 2006;291:H1731–H1737.
32. Castelain V, Herve P, Lecarpentier Y, Duroux P, Simonneau G, Chemla D. Pulmonary artery pulse pressure and wave reflection in chronic pulmonary thromboembolism and primary pulmonary hypertension. *J Am Coll Cardiol*. 2001;37:1085–1092.
33. Ewalenko P, Stefanidis C, Holoye A, Brimiouille S, Naeije R. Pulmonary vascular impedance vs. resistance in hypoxic and hyperoxic dogs: effects of propofol and isoflurane. *J Appl Physiol*. 1993;74:2188–2193.
34. Fourie PR, Coetzee AR. Effect of compliance on a time-domain estimate of the characteristic impedance of the pulmonary artery during acute pulmonary hypertension. *Med Biol Eng Comput*. 1993;31:468–474.
35. Ha B, Lucas CL, Henry GW, Frantz EG, Ferreira JI, Wilcox BR. Effects of chronically elevated pulmonary arterial pressure and flow on right ventricular afterload. *Am J Physiol*. 1994;267:H155–H165.
36. Lambermont B, D'Orio V, Gerard P, Kolh P, Detry O, Marcelle R. Time domain method to identify simultaneously parameters of the windkessel model applied to the pulmonary circulation. *Arch Physiol Biochem*. 1998;106:245–252.
37. Lieber BB, Li Z, Grant BJ. Beat-by-beat changes of viscoelastic and inertial properties of the pulmonary arteries. *J Appl Physiol*. 1994;76:2348–2355.
38. O'Rourke MF, Yaginuma T, Avolio AP. Physiological and pathophysiological implications of ventricular/vascular coupling. *Ann Biomed Eng*. 1984;12:119–134.
39. Pagnamenta A, Bouckaert Y, Wauthy P, Brimiouille S, Naeije R. Continuous versus pulsatile pulmonary hemodynamics in canine oleic acid lung injury. *Am J Respir Crit Care Med*. 2000;162:936–940.
40. Zuckerman BD, Orton EC, Latham LP, Barbieri CC, Stenmark KR, Reeves JT. Pulmonary vascular impedance and wave reflections in the hypoxic calf. *J Appl Physiol*. 1992;72:2118–2127.
41. Mahapatra S, Nishimura RA, Sorajja P, Cha S, McGoon MD. Relationship of pulmonary arterial capacitance and mortality in idiopathic pulmonary arterial hypertension. *J Am Coll Cardiol*. 2006;47:799–803.
42. Chen CH, Nakayama M, Nevo E, Fetis B, Maughan WL, Kass DA. Coupled systolic-ventricular and vascular stiffening with age: implications for pressure regulation and cardiac reserve in the elderly. *J Am Coll Cardiol*. 1998;32:1221–1227.
43. Cho PW, Levin HR, Curtis WE, Tsitlik JE, DiNatale JM, Kass DA, Gardner TJ, Kunel RW, Acker MA. Pressure-volume analysis of changes in cardiac function in chronic cardiomyoplasty. *Ann Thorac Surg*. 1993;56:38–45.
44. Kass DA. Age-related changes in ventricular-arterial coupling: pathophysiological implications. *Heart Fail Rev*. 2002;7:51–62.
45. Kass DA. Clinical evaluation of left heart function by conductance catheter technique. *Eur Heart J*. 1992;13(suppl E):57–64.
46. Kass DA, Midei M, Graves W, Brinker JA, Maughan WL. Use of a conductance (volume) catheter and transient inferior vena caval occlusion for rapid determination of pressure-volume relationships in man. *Cathet Cardiovasc Diagn*. 1988;15:192–202.
47. Kelly RP, Ting CT, Yang TM, Liu CP, Maughan WL, Chang MS, Kass DA. Effective arterial elastance as index of arterial vascular load in humans. *Circulation*. 1992;86:513–521.
48. Lee WS, Nakayama M, Huang WP, Chiou KR, Wu CC, Nevo E, Fetis B, Kass DA, Ding PY, Chen CH. Assessment of left ventricular end-systolic elastance from aortic pressure-left ventricular volume relations. *Heart Vessels*. 2002;16:99–104.
49. Liu CP, Ting CT, Yang TM, Chen JW, Chang MS, Maughan WL, Lawrence W, Kass DA. Reduced left ventricular compliance in human mitral stenosis: role of reversible internal constraint. *Circulation*. 1992;85:1447–1456.
50. Nussbacher A, Gerstenblith G, O'Connor FC, Becker LC, Kass DA, Schulman SP, Fleg JL, Lakatta EG. Hemodynamic effects of unloading the old heart. *Am J Physiol*. 1999;277:H1863–H1871.
51. Pak PH, Kass DA. Assessment of ventricular function in dilated cardiomyopathies. *Curr Opin Cardiol*. 1995;10:339–344.
52. O'Rourke MF, Safar ME. Relationship between aortic stiffening and microvascular disease in brain and kidney: cause and logic of therapy. *Hypertension*. 2005;46:200–204.
53. Montalescot G, Drobinski G, Meurin P, Maclouf J, Sotirov I, Philippe F, Choussat R, Morin E, Thomas D. Effects of prostacyclin on the pulmonary vascular tone and cardiac contractility of patients with pulmonary hypertension secondary to end-stage heart failure. *Am J Cardiol*. 1998;82:749–755.
54. Hemnes AR, Zaiman A, Champion HC. PDE5A inhibition attenuates bleomycin-induced pulmonary fibrosis and pulmonary hypertension through inhibition of ROS generation and RhoA/Rho kinase activation. *Am J Physiol Lung Cell Mol Physiol*. 2008;294:L24–L33.
55. Takimoto E, Belardi D, Tocchetti CG, Vahebi S, Cormaci G, Ketner EA, Moens AL, Champion HC, Kass DA. Compartmentalization of cardiac beta-adrenergic inotropy modulation by phosphodiesterase type 5. *Circulation*. 2007;115:2159–2167.
56. Takimoto E, Champion HC, Belardi D, Moslehi J, Mongillo M, Mergia E, Montrose DC, Isoda T, Aufiero K, Zaccolo M, Dostmann WR, Smith CJ, Kass DA. cGMP catabolism by phosphodiesterase 5A regulates cardiac adrenergic stimulation by NOS3-dependent mechanism. *Circ Res*. 2005;96:100–109.
57. Takimoto E, Champion HC, Li M, Belardi D, Ren S, Rodriguez ER, Bedja D, Gabrielson KL, Wang Y, Kass DA. Chronic inhibition of cyclic GMP phosphodiesterase 5A prevents and reverses cardiac hypertrophy. *Nat Med*. 2005;11:214–222.
58. Allanore Y, Meune C, Vignaux O, Weber S, Legmann P, Kahan A. Bosentan increases myocardial perfusion and function in systemic sclerosis: a magnetic resonance imaging and tissue-Doppler echography study. *J Rheumatol*. 2006;33:2464–2469.
59. Motte S, McEntee K, Naeije R. Endothelin receptor antagonists. *Pharmacol Ther*. 2006;110:386–414.
60. Packer M, McMurray J, Massie BM, Caspi A, Charlon V, Cohen-Solal A, Kiowski W, Kostuk W, Krum H, Levine B, Rizzon P, Soler J, Swedberg K, Anderson S, Demets DL. Clinical effects of endothelin receptor antagonist with bosentan in patients with severe chronic heart failure: results of a pilot study. *J Card Fail*. 2005;11:12–20.
61. Daniels LB, Krummen DE, Blanchard DG. Echocardiography in pulmonary vascular disease. *Cardiol Clin*. 2004;22:383–399, vi.
62. Syeed R, Reeves JT, Welsh D, Raesid D, Johnson MK, Peacock AJ. The relationship between the components of pulmonary artery pressure remains constant under all conditions in both health and disease. *Chest*. 2008;133:633–639.
63. Chemla D, Castelain V, Humbert M, Hebert JL, Simonneau G, Lecarpentier Y, Herve P. New formula for predicting mean pulmonary artery pressure using systolic pulmonary artery pressure. *Chest*. 2004;126:1313–1317.
64. Farzaneh-Far R, Na B, Whooley MA, Schiller NB. Usefulness of non-invasive estimate of pulmonary vascular resistance to predict mortality, heart failure, and adverse cardiovascular events in patients with stable coronary artery disease (from the Heart and Soul Study). *Am J Cardiol*. 2008;101:762–766.
65. Bidart CM, Abbas AE, Parish JM, Chaliki HP, Moreno CA, Lester SJ. The noninvasive evaluation of exercise-induced changes in pulmonary artery pressure and pulmonary vascular resistance. *J Am Soc Echocardiogr*. 2007;20:270–275.
66. Berger M, Haimowitz A, Van Tosh A, Berdoff RL, Goldberg E. Quantitative assessment of pulmonary hypertension in patients with tricuspid regurgitation using continuous wave Doppler ultrasound. *J Am Coll Cardiol*. 1985;6:359–365.
67. Currie PJ, Seward JB, Chan KL, Fyfe DA, Hagler DJ, Mair DD, Reeder GS, Nishimura RA, Tajik AJ. Continuous wave Doppler determination of right ventricular pressure: a simultaneous Doppler-catheterization study in 127 patients. *J Am Coll Cardiol*. 1985;6:750–756.
68. Denton CP, Cailles JB, Phillips GD, Wells AU, Black CM, Bois RM. Comparison of Doppler echocardiography and right heart catheterization to assess pulmonary hypertension in systemic sclerosis. *Br J Rheumatol*. 1997;36:239–243.
69. Hinderliter AL, Willis PW IV, Barst RJ, Rich S, Rubin LJ, Badesch DB, Groves BM, McGoon MD, Tapson VF, Bourge RC, Brundage BH, Koerner SK, Langleben D, Keller CA, Murali S, Uretsky BF, Koch G, Li S, Clayton LM, Jobsis MM, Blackburn SD Jr, Crow JW, Long WA. Effects of long-term infusion of prostacyclin (epoprostenol) on echocardiographic measures of right ventricular structure and function in primary pulmonary hypertension: Primary Pulmonary Hypertension Study Group. *Circulation*. 1997;95:1479–1486.

70. Raymond RJ, Hinderliter AL, Willis PW, Ralph D, Caldwell EJ, Williams W, Ettinger NA, Hill NS, Summer WR, de Boisblanc B, Schwartz T, Koch G, Clayton LM, Jobsis MM, Crow JW, Long W. Echocardiographic predictors of adverse outcomes in primary pulmonary hypertension. *J Am Coll Cardiol*. 2002;39:1214–1219.
71. Fisher MR, Mathai SC, Champion HC, Girgis RE, Houston-Harris T, Hummers L, Krishnan JA, Wigley F, Hassoun PM. Clinical differences between idiopathic and scleroderma-related pulmonary hypertension. *Arthritis Rheum*. 2006;54:3043–3050.
72. Grunig E, Janssen B, Mereles D, Barth U, Borst MM, Vogt IR, Fischer C, Olschewski H, Kuecherer HF, Kubler W. Abnormal pulmonary artery pressure response in asymptomatic carriers of primary pulmonary hypertension gene. *Circulation*. 2000;102:1145–1150.
73. Hopkins SR, Schoene RB, Henderson WR, Spragg RG, Martin TR, West JB. Intense exercise impairs the integrity of the pulmonary blood-gas barrier in elite athletes. *Am J Respir Crit Care Med*. 1997;155:1090–1094.
74. West JB. Left ventricular filling pressures during exercise: a cardiologic blind spot? *Chest*. 1998;113:1695–1697.
75. Rich S, McLaughlin VV. Pulmonary hypertension. In: Braunwald E, ed. In: Braunwald E, ed. *Braunwald's Heart Disease: A Textbook of Cardiovascular Medicine*. 8th ed. Philadelphia, Pa: Saunders Elsevier; 2007: 1883–1913.
76. Apfel HD, Shen Z, Gopal AS, Vangi V, Solowiejczyk D, Altmann K, Barst RJ, Boxt LM, Allan LD, King DL. Quantitative three dimensional echocardiography in patients with pulmonary hypertension and compressed left ventricles: comparison with cross sectional echocardiography and magnetic resonance imaging. *Heart*. 1996;76:350–354.
77. Tei C, Dujardin KS, Hodge DO, Bailey KR, McGoon MD, Tajik AJ, Seward SB. Doppler echocardiographic index for assessment of global right ventricular function. *J Am Soc Echocardiogr*. 1996;9:838–847.
78. Borges AC, Knebel F, Eddicks S, Panda A, Schattke S, Witt C, Baumann G. Right ventricular function assessed by two-dimensional strain and tissue Doppler echocardiography in patients with pulmonary arterial hypertension and effect of vasodilator therapy. *Am J Cardiol*. 2006;98:530–534.
79. Pirat B, McCulloch ML, Zoghbi WA. Evaluation of global and regional right ventricular systolic function in patients with pulmonary hypertension using a novel speckle tracking method. *Am J Cardiol*. 2006;98: 699–704.
80. Moustapha A, Lim M, Saikia S, Kaushik V, Kang SH, Barasch E. Interrogation of the tricuspid annulus by Doppler tissue imaging in patients with chronic pulmonary hypertension: implications for the assessment of right-ventricular systolic and diastolic function. *Cardiology*. 2001;95: 101–104.
81. Meluzin J, Spinarova L, Bakala J, Toman J, Krejci J, Hude P, Kara T, Soucek M. Pulsed Doppler tissue imaging of the velocity of tricuspid annular systolic motion; a new, rapid, and non-invasive method of evaluating right ventricular systolic function. *Eur Heart J*. 2001;22: 340–348.
82. Forfia PR, Fisher MR, Mathai SC, Houston-Harris T, Hemnes AR, Borlaug BA, Chamera E, Corretti MC, Champion HC, Abraham TP, Girgis RE, Hassoun PM. Tricuspid annular displacement predicts survival in pulmonary hypertension. *Am J Respir Crit Care Med*. 2006; 174:1034–1041.
83. Gan CT, Holverda S, Marcus JT, Paulus WJ, Marques KM, Bronzwaer JG, Twisk JW, Boonstra A, Postmus PE, Vonk-Noordegraaf A. Right ventricular diastolic dysfunction and the acute effects of sildenafil in pulmonary hypertension patients. *Chest*. 2007;132:11–17.
84. Stessel H, Brunner F. Effect of endothelin antagonism on contractility, intracellular calcium regulation and calcium regulatory protein expression in right ventricular hypertrophy of the rat. *Basic Clin Pharmacol Toxicol*. 2004;94:37–45.
85. Guazzi M, Pepi M, Maltagliati A, Celeste F, Muratori M, Tamborini G. How the two sides of the heart adapt to graded impedance to venous return with head-up tilting. *J Am Coll Cardiol*. 1995;26:1732–1740.
86. Wilson N, Goldberg SJ, Dickinson DF, Scott O. Normal intracardiac and great artery blood velocity measurements by pulsed Doppler echocardiography. *Br Heart J*. 1985;53:451–458.
87. Kitabatake A, Inoue M, Asao M, Masuyama T, Tanouchi J, Morita T, Mishima M, Uematsu M, Shimazu T, Hori M, Abe H. Noninvasive evaluation of pulmonary hypertension by a pulsed Doppler technique. *Circulation*. 1983;68:302–309.
88. Dabestani A, Mahan G, Gardin JM, Takenaka K, Burn C, Allfie A, Henry WL. Evaluation of pulmonary artery pressure and resistance by pulsed Doppler echocardiography. *Am J Cardiol*. 1987;59:662–668.
89. Boxt LM, Katz J, Kolb T, Czegledy FP, Barst RJ. Direct quantitation of right and left ventricular volumes with nuclear magnetic resonance imaging in patients with primary pulmonary hypertension. *J Am Coll Cardiol*. 1992;19:1508–1515.
90. Katz J, Whang J, Boxt LM, Barst RJ. Estimation of right ventricular mass in normal subjects and in patients with primary pulmonary hypertension by nuclear magnetic resonance imaging. *J Am Coll Cardiol*. 1993;21:1475–1481.
91. Lorenz CH, Walker ES, Morgan VL, Klein SS, Graham TP Jr. Normal human right and left ventricular mass, systolic function, and gender differences by cine magnetic resonance imaging. *J Cardiovasc Magn Reson*. 1999;1:7–21.
92. Hill JM, Dick AJ, Raman VK, Thompson RB, Yu ZX, Hinds KA, Pessanha BS, Guttman MA, Varney TR, Martin BJ, Dunbar CE, McVeigh ER, Lederman RJ. Serial cardiac magnetic resonance imaging of injected mesenchymal stem cells. *Circulation*. 2003;108:1009–1014.
93. Ohno Y, Hatabu H, Murase K, Higashino T, Nogami M, Yoshikawa T, Sugimura K. Primary pulmonary hypertension: 3D dynamic perfusion MRI for quantitative analysis of regional pulmonary perfusion. *AJR Am J Roentgenol*. 2007;188:48–56.
94. Grothues F, Moon JC, Bellenger NG, Smith GS, Klein HU, Pennell DJ. Interstudy reproducibility of right ventricular volumes, function, and mass with cardiovascular magnetic resonance. *Am Heart J*. 2004;147: 218–223.
95. Semelka RC, Tomei E, Wagner S, Mayo J, Caputo G, O'Sullivan M, Parmley WW, Chatterjee K, Wolfe C, Higgins CB. Interstudy reproducibility of dimensional and functional measurements between cine magnetic resonance studies in the morphologically abnormal left ventricle. *Am Heart J*. 1990;119:1367–1373.
96. Saba TS, Foster J, Cockburn M, Cowan M, Peacock AJ. Ventricular mass index using magnetic resonance imaging accurately estimates pulmonary artery pressure. *Eur Respir J*. 2002;20:1519–1524.
97. Roelvelde RJ, Marcus JT, Boonstra A, Postmus PE, Marques KM, Bronzwaer JG, Vonk-Noordegraaf A. A comparison of noninvasive MRI-based methods of estimating pulmonary artery pressure in pulmonary hypertension. *J Magn Reson Imaging*. 2005;22:67–72.
98. van Wolferen SA, Marcus JT, Boonstra A, Marques KM, Bronzwaer JG, Spreeuwenberg MD, Postmus PE, Vonk-Noordegraaf A. Prognostic value of right ventricular mass, volume, and function in idiopathic pulmonary arterial hypertension. *Eur Heart J*. 2007;28:1250–1257.
99. Michelakis ED, Tymchak W, Noga M, Webster L, Wu XC, Lien D, Wang SH, Modry D, Archer SL. Long-term treatment with oral sildenafil is safe and improves functional capacity and hemodynamics in patients with pulmonary arterial hypertension. *Circulation*. 2003;108: 2066–2069.
100. Tardivon AA, Mousseaux E, Brenot F, Bittoun J, Jolivet O, Bourroul E, Duroux P. Quantification of hemodynamics in primary pulmonary hypertension with magnetic resonance imaging. *Am J Respir Crit Care Med*. 1994;150:1075–1080.
101. Kondo C, Caputo GR, Masui T, Foster E, O'Sullivan M, Stulberg MS, Golden J, Catterjee K, Higgins CB. Pulmonary hypertension: pulmonary flow quantification and flow profile analysis with velocity-encoded cine MR imaging. *Radiology*. 1992;183:751–758.
102. Michelakis ED. Spatio-temporal diversity of apoptosis within the vascular wall in pulmonary arterial hypertension: heterogeneous BMP signaling may have therapeutic implications. *Circ Res*. 2006;98: 172–175.
103. Nagendran J, Gurtu V, Fu DZ, Dyck JR, Haromy A, Ross DB, Rebecka IM, Michelakis ED. A dynamic and chamber-specific mitochondrial remodeling in right ventricular hypertrophy can be therapeutically targeted. *J Thorac Cardiovasc Surg*. 2008;136:168–178. 178.e1–178.e3.
104. Zierler K. Indicator dilution methods for measuring blood flow, volume, and other properties of biological systems: a brief history and memoir. *Ann Biomed Eng*. 2000;28:836–848.
105. Hatabu H, Gaa J, Kim D, Li W, Prasad PV, Edelman RR. Pulmonary perfusion: qualitative assessment with dynamic contrast-enhanced MRI using ultra-short TE and inversion recovery turbo FLASH. *Magn Reson Med*. 1996;36:503–508.
106. Hatabu H, Tadamura E, Levin DL, Chen Q, Li W, Kim D, Prasad PV, Edelman RR. Quantitative assessment of pulmonary perfusion with dynamic contrast-enhanced MRI. *Magn Reson Med*. 1999;42: 1033–1038.

107. Levin DL, Chen Q, Zhang M, Edelman RR, Hatabu H. Evaluation of regional pulmonary perfusion using ultrafast magnetic resonance imaging. *Magn Reson Med*. 2001;46:166–171.
108. Uematsu H, Levin DL, Hatabu H. Quantification of pulmonary perfusion with MR imaging: recent advances. *Eur J Radiol*. 2001;37:155–163.
109. Ohno Y, Hatabu H, Murase K, Higashino T, Kawamitsu H, Watanabe H, Takenaka D, Fujii M, Sugimura K. Quantitative assessment of regional pulmonary perfusion in the entire lung using three-dimensional ultrafast dynamic contrast-enhanced magnetic resonance imaging: preliminary experience in 40 subjects. *J Magn Reson Imaging*. 2004;20:353–365.
110. Ohno Y, Murase K, Higashino T, Nogami M, Koyama H, Takenaka D, Kawamitsu H, Matsumoto S, Hatabu H, Sugimura K. Assessment of bolus injection protocol with appropriate concentration for quantitative assessment of pulmonary perfusion by dynamic contrast-enhanced MR imaging. *J Magn Reson Imaging*. 2007;25:55–65.
111. Kuehne T, Yilmaz S, Steendijk P, Moore P, Groenink M, Saaed M, Weber O, Higgins CB, Ewert P, Fleck E, Nagel E, Schulze-Neick I, Lange P. Magnetic resonance imaging analysis of right ventricular pressure-volume loops: in vivo validation and clinical application in patients with pulmonary hypertension. *Circulation*. 2004;110:2010–2016.
112. Laufer EM, Reutelingsperger CP, Narula J, Hofstra L. Annexin A5: an imaging biomarker of cardiovascular risk. *Basic Res Cardiol*. 2008;103:95–104.
113. Kietselaer BL, Reutelingsperger CP, Heidendal GA, Daemen MJ, Mess WH, Hofstra L, Narula J. Noninvasive detection of plaque instability with use of radiolabeled annexin A5 in patients with carotid-artery atherosclerosis. *N Engl J Med*. 2004;350:1472–1473.
114. Sosnovik DE, Schellenberger EA, Nahrendorf M, Novikov MS, Matsui T, Dai G, Reynolds F, Grazette L, Rosenzweig A, Weissleder R, Josephson L. Magnetic resonance imaging of cardiomyocyte apoptosis with a novel magneto-optical nanoparticle. *Magn Reson Med*. 2005;54:718–724.
115. Kim JW, Dang CV. Multifaceted roles of glycolytic enzymes. *Trends Biochem Sci*. 2005;30:142–150.
116. Kim JW, Dang CV. Cancer's molecular sweet tooth and the Warburg effect. *Cancer Res*. 2006;66:8927–8930.
117. Bonnet S, Archer SL, Allalunis-Turner J, Haromy A, Beaulieu C, Thompson R, Lee CT, Lopaschuk GD, Puttagunta L, Bonnet S, Harry G, Hashimoto K, Porter CJ, Andrade MA, Thebaud B, Michelakis ED. A mitochondria-K<sup>+</sup> channel axis is suppressed in cancer and its normalization promotes apoptosis and inhibits cancer growth. *Cancer Cell*. 2007;11:37–51.
118. McMurtry MS, Bonnet S, Wu X, Dyck JR, Haromy A, Hashimoto K, Michelakis ED. Dichloroacetate prevents and reverses pulmonary hypertension by inducing pulmonary artery smooth muscle cell apoptosis. *Circ Res*. 2004;95:830–840.
119. Xu W, Koeck T, Lara AR, Neumann D, DiFilippo FP, Koo M, Janocha AJ, Masri FA, Arroliga AC, Jennings C, Dweik RA, Tudor RM, Stuehr DJ, Erzurum SC. Alterations of cellular bioenergetics in pulmonary artery endothelial cells. *Proc Natl Acad Sci U S A*. 2007;104:1342–1347.
120. de las Fuentes L, Herrero P, Peterson LR, Kelly DP, Gropler RJ, Davila-Roman VG. Myocardial fatty acid metabolism: independent predictor of left ventricular mass in hypertensive heart disease. *Hypertension*. 2003;41:83–87.
121. Yonekura Y, Brill AB, Som P, Yamamoto K, Srivastava SC, Iwai J, Elmaleh DR, Livni E, Strauss HW, Goodman MM, Knapp FF. Regional myocardial substrate uptake in hypertensive rats: a quantitative autoradiographic measurement. *Science*. 1985;227:1494–1496.
122. Beslija S, Bonnetterre J, Burstein H, Cocquyt V, Gnant M, Goodwin P, Heinemann V, Jassem J, Kostler WJ, Krainer M, Menard S, Petit T, Petruzella L, Possinger K, Schmid P, Stadtmayer E, Stockler M, Van Belle S, Vogel C, Wilcken N, Wiltshchke C, Zielinski CC, Zwierzina H. Second consensus on medical treatment of metastatic breast cancer. *Ann Oncol*. 2007;18:215–225.
123. Takeyama D, Kagaya Y, Yamane Y, Shiba N, Chida M, Takahashi T, Ido T, Ishide N, Takishima T. Effects of chronic right ventricular pressure overload on myocardial glucose and free fatty acid metabolism in the conscious rat. *Cardiovasc Res*. 1995;29:763–767.
124. Gambhir SS. Molecular imaging of cancer with positron emission tomography. *Nat Rev Cancer*. 2002;2:683–693.
125. Oikawa M, Kagaya Y, Otani H, Sakuma M, Demachi J, Suzuki J, Takahashi T, Nawata J, Ido T, Watanabe J, Shirato K. Increased [<sup>18</sup>F]fluorodeoxyglucose accumulation in right ventricular free wall in patients with pulmonary hypertension and the effect of epoprostenol. *J Am Coll Cardiol*. 2005;45:1849–1855.

KEY WORDS: diagnosis ■ echocardiography ■ lung ■ magnetic resonance imaging ■ pulmonary heart disease